J. Anat. (1999) **195**, pp. 101–110, with 5 figures Printed in the United Kingdom

The electron microscope appearance of the subchondral bone plate in the human femoral head in osteoarthritis and osteoporosis

BAOHUA LI[1], DEBORAH MARSHALL[2], MARTIN ROE[3] AND RICHARD M. ASPDEN[1]

[1] *Department of Orthopaedics and* [2] *Foresterhill Electron Microscopy Unit, Department of Medical Microbiology, University of Aberdeen, and* [3] *Soils Group, Macaulay Land Use Research Institute, Aberdeen, UK*

(*Accepted 23 March 1999*)

ABSTRACT

The subchondral bone plate supports the articular cartilage in diarthrodial joints. It has a significant mechanical function in transmitting loads from the cartilage into the underlying cancellous bone and has been implicated in the destruction of cartilage in osteoarthritis (OA) and its sparing in osteoporosis (OP), but little is known of its composition, structure or material properties. This study investigated the microscopic appearance and mineral composition of the subchondral bone plate in femoral heads from patients with OA or OP to determine how these correspond to changes in composition and stiffness found in other studies. Freeze-fractured full-depth samples of the subchondral bone plate from the femoral heads of patients with osteoarthritis, osteoporosis or a matched control group were examined using back scattered and secondary emission scanning electron microscopy. Other samples were embedded and polished and examined using back-scattered electron microscopy and electron probe microanalysis. The appearances of the samples from the normal and osteoporotic patients were very similar, with the subchondral bone plate overlayed by a layer of calcified cartilage. Osteoporotic samples presented a more uniform fracture surface and the relative thicknesses of the layers appeared to be different. In contrast, the OA bone plate appeared to be porous and have a much more textured surface. There were occasional sites of microtrabecular bone formation between the trabeculae of the underlying cancellous bone, which were not seen in the other groups, and more numerous osteoclast resorption pits. The calcified cartilage layer was almost absent and the bone plate was apparently thickened. The appearance of the osteoarthritic subchondral bone plate was, therefore, considerably different from both the normal and the osteoporotic, strongly indicative of abnormal cellular activity.

Key words: Joints; articular cartilage.

INTRODUCTION

The subchondral bone plate is a layer of dense bone underlying the articular cartilage in synovial joints. It forms the main supporting structure for the cartilage and transmits loads from the cartilage into the cancellous bone beneath. The importance of the interface between articular cartilage and bone has long been recognised, especially with regard to the transfer of stress from the compliant matrix of cartilage to the considerably stiffer bone, and the calcified layer of the cartilage is believed to act as an intermediate in this respect (Redler et al. 1975; Clark & Huber, 1990; Mente & Lewis, 1994). However, less seems to be known of the structure and behaviour of the subchondral bone plate.

Sclerosis of the subchondral bone is a well recognised clinical feature of osteoarthritis (OA) and many studies have been made of morphometric parameters such as trabecular thickness and orientation (e.g. Christensen et al. 1982; Simkin et al. 1991; Shimizu et al. 1993; Kamibayashi et al. 1995*a*, *b*), and

Correspondence to Dr R. M. Aspden, Department of Orthopaedics, University of Aberdeen, Polwarth Building, Foresterhill, Aberdeen AB25 2ZD. Tel: +44 (0)1224 681818, ext. 53007; fax: +44 (0)1224 685373; e-mail r.aspden@abdn.ac.uk

bone apposition rates in health and disease (Walton & Elves, 1979; Amir et al. 1992). Fewer studies appear to have concentrated on the subchondral bone plate itself, but measurements have shown it to thicken in animals subjected to strenuous exercise (Oettmeier et al. 1992) and following derangement of a joint (Dedrick et al. 1993). Site variation studies have shown a greater thickness of the subchondral bone plate plus the overlying mineralised cartilage, which together were referred to as the subchondral plate, in more heavily loaded regions in the tibial plateau and the patella (Milz & Putz, 1994; Milz et al. 1995). It is also reported that there is a thickening of the subchondral plate in OA in humans (Chai et al. 1991; Dedrick et al. 1993) and animals (Carlson et al. 1996), although another study found little change in the combined thickness of the bone plate and mineralised cartilage, called the subchondral mineralised zone (SMZ), under cartilage lesions in patellae (Eckstein et al. 1998). There was, however, a difference between males and females (Eckstein et al. 1998). There appears to be little change, or perhaps even a slight decrease, in mechanical properties as measured using indentation tests (Lereim et al. 1974; Björkström & Goldie, 1982) or ultrasound (Li & Aspden, 1997*a*) in subchondral bone plate from patients with OA.

The role of the subchondral bone, especially the subchondral bone plate, in OA is a matter of some debate. Traditionally, it has been accepted that changes in the subchondral bone are secondary to the primary disease process which is believed to occur in the articular cartilage. Degeneration and erosion of the articular cartilage then result in mechanical overloading of the bone which responds by becoming sclerotic, leading, in turn, to further degeneration in the cartilage. However, a number of recent studies have found changes in the bone that are not readily explicable by this model of the disease (Mbuyi-Muamba & Dequeker, 1984; Gevers et al. 1989; Dequeker et al. 1995; Li & Aspden, 1997*b*). Evidence is slowly accumulating that changes may be seen in the bone early in the disease process (Bailey & Mansell, 1997; Petersson et al. 1998) and it has been hypothesised that stiffening of the underlying bone could result in secondary damage to the cartilage and OA (Radin & Rose, 1986). The idea has been supported by the converse observation that OA is rare in patients with osteoporosis (OP), and this is attributed to a weakening of the subchondral bone which is thought to protect the cartilage (Dequeker et al. 1995). While conceptually plausible, little experimental evidence has accrued to confirm the role of the subchondral bone in these mechanisms, and recent studies by Gevers et al. (1989) Mbuyi-Muamba & Dequeker (1984), Dequeker et al. (1995) and Li & Aspden (1997*b*) are not fully consistent with the traditional model of the disease. Our recent study of the mechanical and material properties of the subchondral bone plate indicated that although its thickness increases in OA femoral heads, its stiffness, the density of the bone and the mass fraction of mineral are all reduced (Li & Aspden, 1997*a*). In contrast, the subchondral bone plate from patients with osteoporosis (OP) was thinner and less stiff than normal but had very similar composition and density. These unexpected results led to the study described here which investigates the appearance of the subchondral bone plate in femoral heads from patients with OA or OP. Electron microscopy, using both back-scattered (BSE) and secondary (SE) electron imaging, and quantitative electron probe microanalysis (EPMA) were used to determine whether the changes described above were matched by alterations in the microscopic appearance and mineral composition of the bone.

MATERIALS AND METHODS

Femoral heads from 3 clinical groups, OA, OP and normal, were collected and matched for age (median 72 y, range 68–76) and sex. Femoral heads from OA patients were obtained in the operating theatre after elective total hip replacement; those from OP patients after hemiarthroplasty for a fractured neck of femur caused by a fall and attributed to OP. Cases with osteomalacia, multiple myeloma, rheumatoid arthritis, or secondary osteoporosis due to corticosteroids were excluded from the osteoporotic group. Patients with rheumatoid arthritis, congenital or acquired dysplasia, gout, or avascular necrosis were excluded from the osteoarthritic group. A control group was collected from hips removed during postmortem examination and the medical records were examined to exclude disorders affecting bone metabolism. All samples were stored at 4 °C in a calcium phosphate buffered 0.15 M saline solution containing sodium azide (Li & Aspden, 1997*b*) as this has been shown to preserve the structure and composition of the bone (Lees, 1988). A cortical bone sample was obtained from the midshaft of the femur from one normal control for comparison.

Subchondral bone plate samples from 7 femoral heads in each group were prepared for scanning electron microscopy (SEM). Cores, 9 mm in diameter and about 10 mm deep, were removed from the

superior and inferior regions of each femoral head as described in detail elsewhere (Li & Aspden, 1997*b*). These areas correspond to heavily and lightly loaded regions (Thomas & Daniel, 1983; Hodge et al. 1986) and enable a comparison to be made of the possible effects of load bearing. When present, most of the depth of the articular cartilage was removed using a scalpel, but care was taken not to damage the surface of the bone. The subchondral plate was removed with about 1 mm of cancellous bone using a mineralogical saw (Struers Accutom-2) fitted with an aluminium oxide cut-off wheel rotating at 300 rpm and cooled with distilled water. Remaining soft tissue and other organic material was removed by digestion with proteinase K (1 mg/ml) and detergent (sodium dodecyl sulphate, SDS, 1% w/v) at 37 °C for 48 h. Previous studies have shown that this effectively removes all organic material from the surfaces of trabecular bone but has no noticeable effect on the collagen comprising the bone matrix itself (Murali et al. 1994). They were then washed in distilled water for 6 h.

Freeze-fractured SEM

Specimens from 5 of the femoral heads in each group, selected at random, were prepared by washing in several changes of acetone over ~ 2 h before being left in acetone for 48 h. They were then washed in several changes of diethyl ether over 24 h. Finally they were placed in an oven at 60 °C for 6 h and left in a vacuum desiccator overnight. Following this a fracture plane was produced in each specimen, perpendicular to the original cartilage surface, by immersing it in liquid nitrogen and then bending it using forceps. This was to avoid artefacts that might be produced if the bone was cut or sectioned, and the nature of the fracture surface should yield information on the material properties. Residual vapours were removed by placing in a vacuum down to 10^{-5} mbar before mounting on aluminium stubs using colloidal silver adhesive for examination in a JEOL JSM-35CF scanning electron microscope. Each specimen was examined first in back-scattered mode (BSE) at an accelerating voltage of 30 kV. It was then coated with 20 nm platinum and re-examined in secondary electron (SE) mode at an accelerating voltage of 10 kV. Identifiable landmarks enabled the same areas to be compared by imaging them at the same magnifications using both modalities.

Quantitative electron microprobe analysis

Contrast in a BSE image is dependent on the mean atomic number of the atoms present (regions of higher average atomic number appearing lighter) but is strongly affected by the surface topography. Because of this, and to perform EPMA, some samples were prepared with a flat polished surface to ensure that any significant observations were not artefacts of the rough fracture surface. Specimens from the remaining 2 femoral heads were prepared for this by embedding the bone in a low-viscosity acrylic resin (LR White) under vacuum to ensure total impregnation. The resin was thermally cured without the need for a catalyst at a temperature of 55 °C for 18–24 h. After curing, each specimen was sectioned using a diamond saw in a plane perpendicular to the subchondral surface of the bone. The cut face was then polished on a lapping machine using silicon carbide lapping plates and successively finer grades of diamond paste. A slab containing the prepared surface, approximately 5 mm thick, was then cut off, mounted on an SEM stub and carbon coated. Samples were examined using a Philips XL20 SEM equipped with Oxford Instruments Link eXLII x-ray system fitted with a Pentafet thin window detector capable of detecting elements down to boron ($Z = 5$) operating in BSE mode with an accelerating voltage of 20 kV.

Electron probe microanalysis measures local elemental composition, with a lateral resolution of ~ 1 μm, by detecting the characteristic x-rays emitted by the atoms when they are irradiated by the electron beam. Each spectrum was recorded over a period of 100 s. Spectra from the bone were recorded with the beryllium window open in the detector, allowing detection of low atomic weight nuclides. The concentrations of the elements calcium, phosphorus and oxygen were obtained by reference to a standard of known concentration. Peak intensities were corrected by the so-called ZAF correction (Z = atomic number, A = an absorption factor and F = a fluorescence factor). Results are expressed as the percentage by weight of the oxides CaO and P_2O_5, based on an assumed valency for each element and the stoichiometry of the mineral, and the ratio of Ca:P. For the purposes of the analysis, this was based on an ideal hydroxyapatite formula containing 25 oxygen atoms per unit cell: $2[Ca_5(PO_4)_3OH]$, 1 oxygen being assumed lost due to beam damage, and in this case the ideal Ca:P ratio is 1.67. The total percentage of oxides is a measure of the amount of material present, the remainder being porosity, and is the conventional mineralogical means of presenting the data. The

spectrum from the surface layer was recorded with the beryllium window closed, to suppress the otherwise very large carbon peak, and without embedding the sample in order to remove a chlorine peak arising from the resin.

RESULTS

Freeze-fractured SEM

No obvious differences were found between samples from the superior and inferior aspects of any of the femoral heads examined and so pictures have been selected to illustrate general features that could be observed in all the samples studied. The appearance of normal subchondral bone plate using BSE imaging can be seen in Figure 1*a* and the corresponding secondary electron image in Figure 1*b*. Most noticeable in the BSE images was the dark layer along the surface. This layer can be seen enlarged in Figure 1*c* and the rougher texture of its fracture surface compared with that of the underlying bone which appears white in a BSE image. An SE image at the same magnification shows more clearly the roughness of the fracture surface and at higher magnification the fibrous nature of the upper layer could be seen (Fig. 1*d*). This figure also shows the interface between the dark and light zones which can be seen to be quite sharp, the texture changing over a distance of only a few micrometres. In contrast, the transition from the bone plate to the cancellous bone was very variable and appeared as a merging together of the trabecular arrangement of the cancellous bone.

The OP bone showed a similar pattern of a dark layer overlying a light layer in BSE images (Fig. 2*a*). However, the fracture surfaces were smoother in both layers (Fig. 2*b–d*) and they also appeared much flatter. The 2 layers can just be distinguished in the corresponding SE image (Fig. 2*b*). Unlike the appearance of normal bone, at high magnification the interface presented 2 different appearances, sometimes in different parts of the same sample: one was relatively featureless with either very fine fibres in the dark layer or fibres masked by mineral (Fig. 2*e*), the other was very similar to normal with clear fibrous texture evident in the dark layer but not in the bone

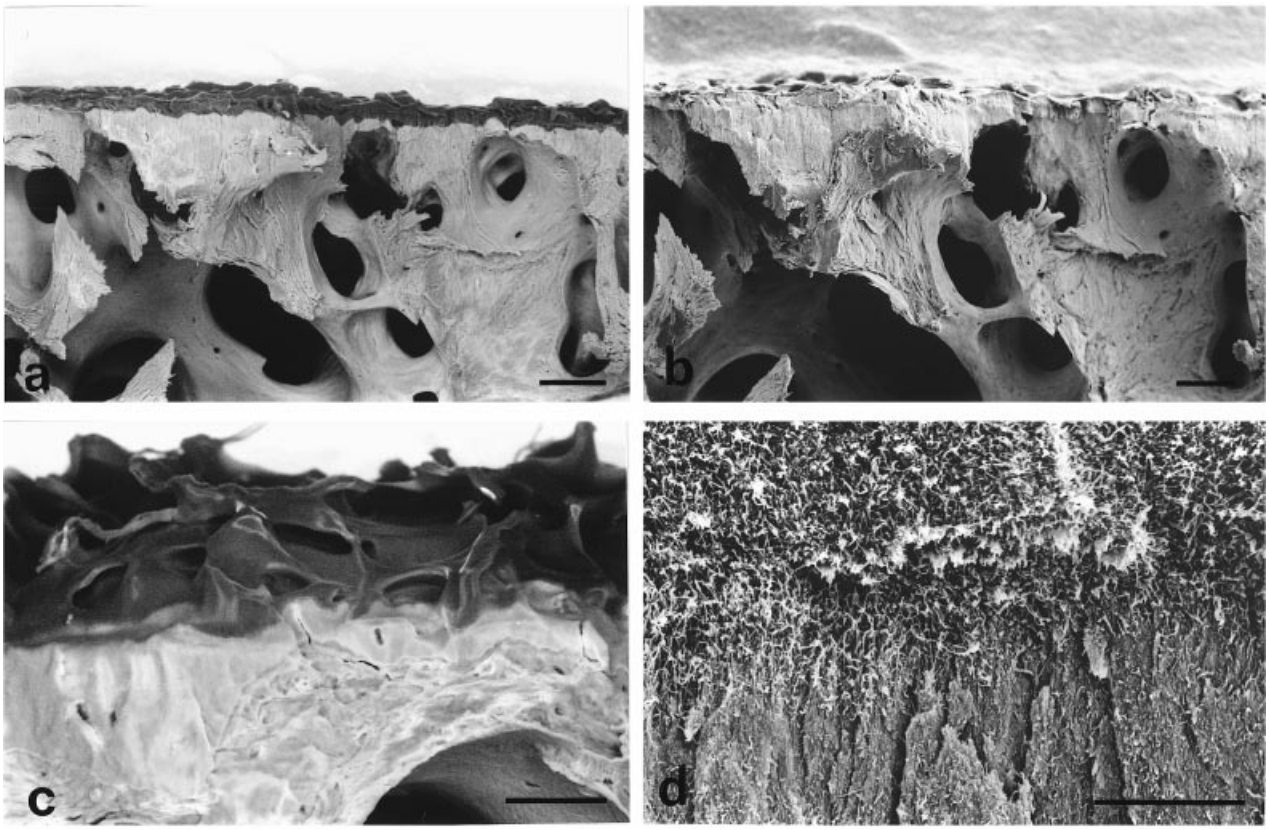

Fig. 1. Electron microscopic appearance of normal subchondral bone plate from a 76-y-old male. (*a*) Back-scattered image and (*b*) corresponding secondary emission image of the fracture surface. Bars, 200 μm. Part of this BS image is enlarged in (*c*) to show the fractured surface of the bone in more detail. Bar, 100 μm. The osteochondral junction between the mineralised cartilage (dark layer) and the bone (light) can be seen at still greater magnification in the SE image (*d*) with the fibrous nature of the dark layer now quite apparent. Bar, 20 μm.

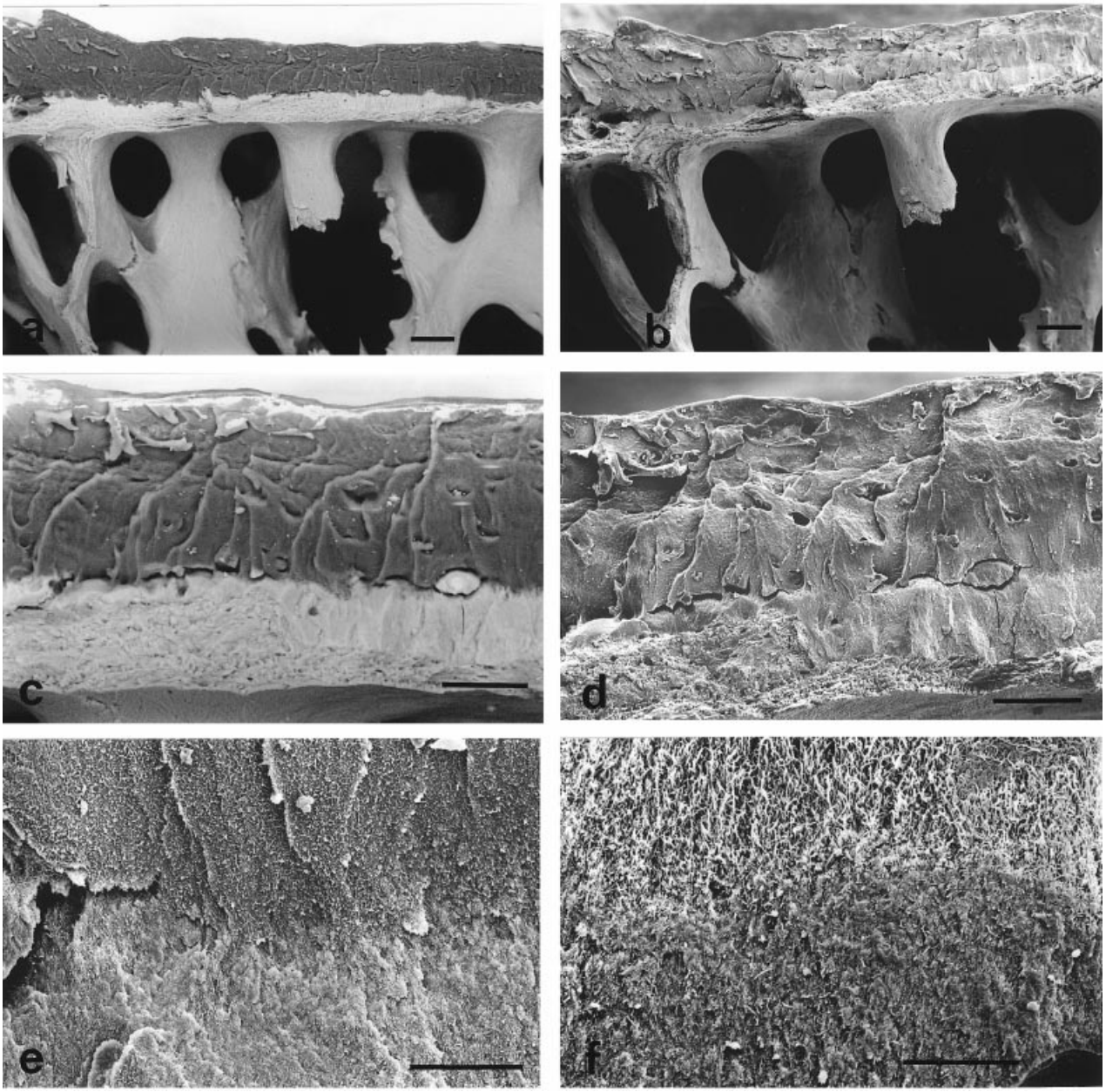

Fig. 2. Electron microscopic appearance of osteoporotic subchondral bone plate from a 76-y-old female. The BS image (*a*), and the corresponding SE image (*b*), show the smoother nature of the fracture surface and the osteochondral junction. Bars, 200 μm. At higher magnifications the facture surface still appears smooth in BS (*c*) and SE images (*d*). Bars, 100 μm. The interface between the 2 layers can be clearly seen at still higher magnification but presented with 2 types of appearance in SE images: one relatively featureless (*e*) and the other similar to normal (*f*). Bars, 20 μm.

(Fig. 2*f*). In both cases, however, the transition was sharp and occurred over only a few micrometres. In all cases the dark layer was thicker than the light layer, in contrast to the appearance of the normal bone.

A number of striking differences could be seen in the OA bone when compared with normal and OP bone. The first was the almost total nonexistence of the dark layer seen in BSE images (Figs 3*a*, *c*). The corresponding SE images can be seen in Figure 3*b* and *d*. Considerably more bone was present, both in the cancellous bone where the trabeculae appeared thicker and merged into one another, and in the subchondral bone plate. Three other features were readily apparent. The first was that the bone appeared to be very porous, on different scales, both over the natural surfaces and in the fractured ends of trabeculae (Fig. 3*b*, *c*, *d*, *e*). At higher magnification (Fig. 3*f*), the diameter of the larger holes can be seen to be $\sim$ 10–20 μm, which is the usual appearance of osteocyte lacunae in forming bone surface (Boyde et al. 1986;

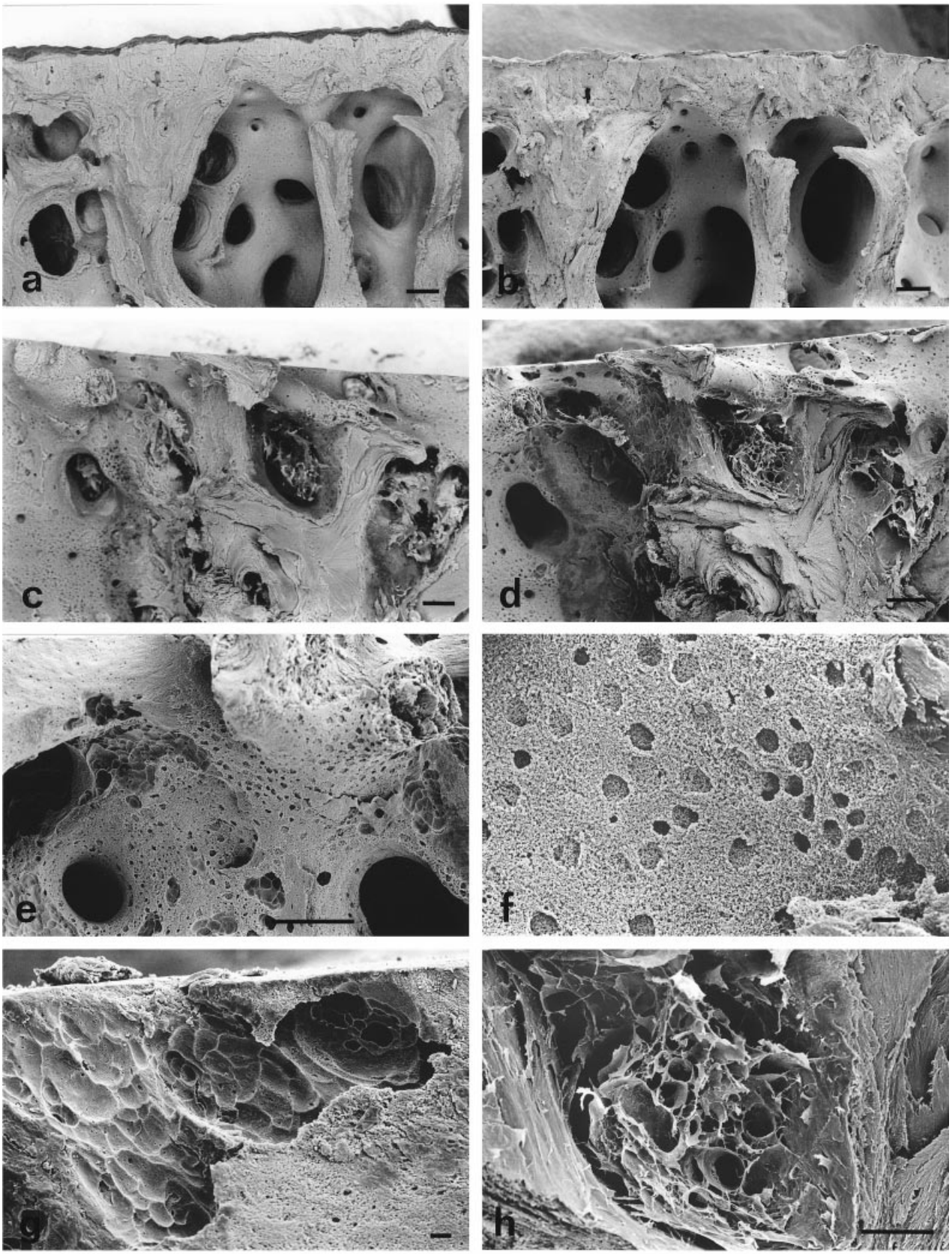

Fig. 3. Osteoarthritic bone appeared markedly different from normal in both BS images ((*a*) from a 75-y-old female and (*c*) from a 70-y-old female) and corresponding SE images (*b*, *d*) with total or almost complete absence of the dark surface layer. Bars, 200 μm. The bone surfaces are penetrated by numerous small holes which can also be seen on the fractured ends of trabeculae (*e*). Bar, 200 μm. At higher magnification (*f*) a finer texture is also apparent. Bar, 20 μm. Howship's lacunae can be seen at numerous sites in (*e*) and at higher magnification at a different site in (*g*). Bar, 20 μm. There is evidence of unusual microtrabecular bone formation in some of the pores (*d*) and at higher magnification in (*h*). Bar, 100 μm. (*e–h* are all SE images.)

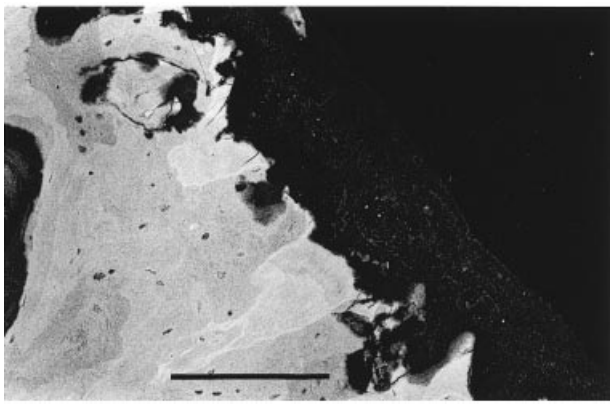

Fig. 4. Samples embedded and polished demonstrated a similar gross appearance in BSE images and are represented here by an image of OA bone. Bar, 200 μm. Islands of slightly different contrast may be seen in the subchondral bone plate, and the total oxide contents of these islands are shown in Table 2.

Jones & Boyde, 1993). There was also a much finer porous texture to the bone, visible over the natural surface, in the back surfaces of the lacunae and on the fracture surfaces of trabeculae, that was never observed in the OP or the normals. Secondly, resorption pits could be seen at numerous discrete sites (Fig. 3*e*, *g*), in considerably greater numbers than observed in OP or normal bone. Finally, there was evidence of unusual bone formation with the appearance of microtrabeculae filling some of the pores (Fig. 3*d*, *h*). That these were mineralised and not just organic remnants is demonstrated both by their remaining after proteinase treatment during specimen preparation and by their appearance in the BSE image; organic matter would not be evident and the white appearance strongly suggests the presence of calcium.

Electron microprobe analysis

The general appearance of polished, embedded samples using BSE imaging was similar to that described above, confirming that the rough topography of the fracture surface had not introduced significant artefacts. Only the normal and OP samples had a notable dark layer at the surface; in the OA samples it was very thin or absent. Islands of slightly different contrast could be seen in the subchondral bone (Fig. 4), especially from the OA and OP groups, reflecting small differences in the amount of mineral present. Electron microprobe analysis of the bone indicated that there was no significant difference between any of the samples in the ratio of calcium to phosphorus (Table 1) and that this was similar to the ratio obtained from cortical bone from the midshaft of the femur. A typical trace is shown in Figure 5*a*. Analysis

Table 1. *Ratio of calcium to phosphorus in the subchondral bone plate from the superior and inferior aspects of the femoral head from different patient groups compared with normal cortical bone*

		Ca/P
Cortical	–	1.65 ± 0.12
Osteoporosis	Superior	1.70 ± 0.08
	Inferior	1.65 ± 0.15
Osteoarthritis	Superior	1.67 ± 0.12
	Inferior	1.70 ± 0.10
Normal	Superior	1.70 ± 0.11
	Inferior	1.69 ± 0.08

* Mean ± standard deviation. Ideal hydroxyapatite would have a ratio of 1.67.

Table 2. *Percentage oxide totals in the subchondral bone plate determined by electron microprobe analysis from superior and inferior aspects of the femoral heads of patients with OA or OP*

Patient group	Aspect	Light	Dark
Osteoporotic	Superior	59.3 ± 2.2	55.4 ± 0.9
	Inferior	59.7 ± 1.4	56.5 ± 1.3
Osteoarthritic	Superior	57.4 ± 3.2	48.8 ± 2.0
	Inferior	59.9 ± 0.9	59.2 ± 3.1
Normal	Superior	57.5 ± 1.0	
	Inferior	58.9 ± 1.7	
Cortical		57.6 ± 1.3	

* 'Light' and 'dark' are descriptions of the appearance of islands within the OA and Op bone seen in BSE images.

by weight of oxide (Table 2) showed that between the lighter and the darker islands the total percentage of oxide varied between about 55 – 60 % in the osteoporotic, with the lighter regions having the higher percentage and, therefore, the greater average atomic number. Values for normal and cortical bone can be seen to fall in the middle of this range. Bone from the superior aspect of the OA femoral head had lower values for both light and dark regions whereas the inferior aspect was much more homogeneous but yielded values at the upper end of the range found in the other bone types.

The dark surface layer in the OP and normal groups showed a very different elemental composition from that of the underlying bone, as may be seen in the spectra of Figure 5. Calcium and phosphorus were still present, though in much smaller concentrations, but there was a also a significant amount of sulphur.

DISCUSSION

This study shows that there are considerable differences in the appearance of the subchondral bone plate

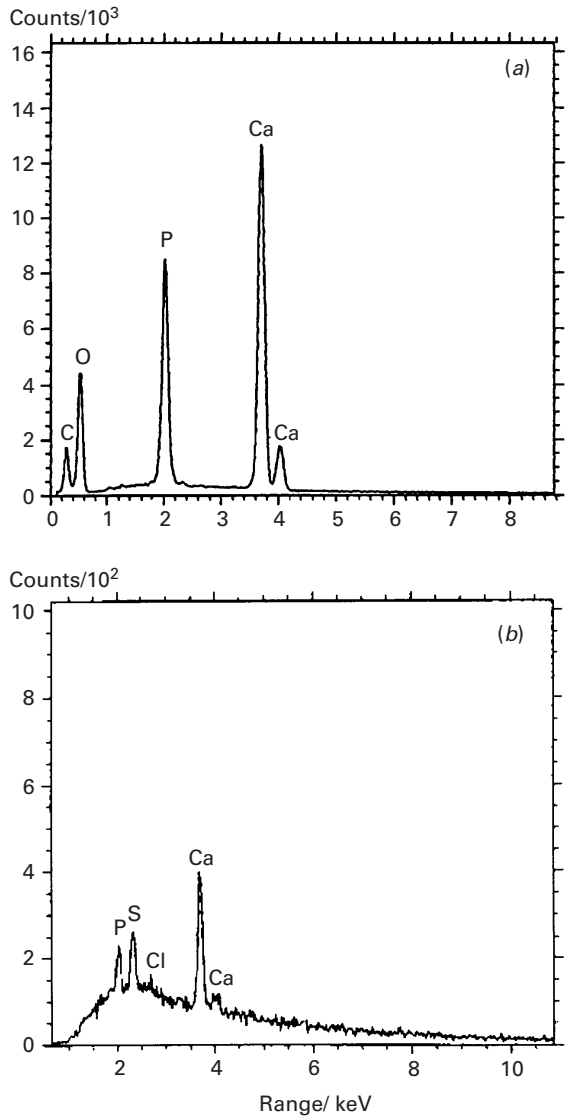

Fig. 5. (*a*) Typical spectrum recorded from the bone plate using electron probe microanalysis (Be window open). (*b*) Typical spectrum recorded from the dark surface layer, with the Be window closed to eliminate the otherwise dominant carbon peak, showing a significant amount of sulphur as well as calcium. There were no significant visible differences in the spectra from the different disease groups.

between the 3 patient groups studied and that the most marked of these are found in the osteoarthritic group. There was little to distinguish the osteoporotic group from the normal group, the most obvious changes being a thinning of the subchondral bone plate and the trabeculae, an apparent increase in the dark surface layer and a smoother fracture surface. This latter could be an indication of an increased tendency towards brittle fracture in which a crack, once initiated, propagates more readily than if the fracture surface being produced is rougher or more irregular. In contrast, the osteoarthritic samples not only demonstrated a thicker subchondral bone plate but contained features that were not present in the other groups.

The overall texture of the OA bone was unlike that of the other groups. The greater number of pores, and visible fibres in the subchondral bone plate itself, together suggest a less firmly compacted structure. This appearance is in qualitative agreement with the results of a quantitative study of the composition and stiffness of the bone plate(Li & Aspden, 1997*a*). This showed a lower density and mineral content and a reduced stiffness, compared with normal bone, and that these changes were not restricted to the bone plate but were found in the cancellous bone throughout the femoral head. The microtrabeculae in Figure 3*d* and *h* are very similar to structures we observed in a previous study of osteoporotic bone in the femoral heads of patients which had been injected with a paste of calcium salts containing growth hormone (Murali et al. 1994). In that case they formed bridges between apatite crystals, and their gradual thickening from the centre of the injected material to the periphery suggested that they formed the early stages of new bone formation which was attempting to repair the defect. In this OA group there is no defect which new bone might be trying to fill so the presence of such a structure is more of a puzzle, but is another indication of abnormal behaviour.

The clusters of resorption pits seen in Figure 3*e* and *g* in the trabecular bone are similar to those described in previous studies (Jones et al. 1984; Jones & Boyde, 1993). These were more plentiful in the OA than in the other patient groups where, in the samples studied, they were not evident. This suggests either a greater number of osteoclasts are active or that the depressions left by the osteoclasts are not being filled as rapidly or effectively. The significance of this is not easy to gauge as without evidence of concurrent osteoblastic activity it is not possible to say whether this represents a greater rate of bone remodelling or simply more bone resorption. However, the massive proliferation of bone found in OA would suggest that osteoblastic activity outweighs that of the osteoclasts, and so it is not clear why more of these lacunae are evident in the OA bone than in either the OP or the normal tissue.

The appearance of the very dark layer on the surface of the normal and OP groups and its x-ray spectrum, showing the presence of significant amounts of sulphur in addition to calcium and phosphorus, suggest that this represents the calcified layer of articular cartilage, in which the sulphur would be present in the sulphated glycosaminoglycans. Removal of most of the articular cartilage with a scalpel

as the first stage of tissue preparation and the enzymic digestion of what remained would leave behind only mineralised tissue. Our previous studies (Murali et al. 1994) have shown that the proteinase treatment used is highly effective at removing unmineralised organic material. The presence of calcium, albeit at lower concentrations than in the bone, shows that this tissue is mineralised. In addition, the undulating morphology of the interface with the subchondral bone plate is very similar to that seen using histology (Meachim & Stockwell, 1979) and described in the definition of the SMZ (Eckstein et al. 1998). The calcified cartilage provides a transition region between the compliant unmineralised cartilage and the stiffer bone and presumably helps to prevent large stress concentrations at the interface. Anchoring a compliant material to a stiff one is not a trivial problem, in biology or engineering, and how the transition is effected and maintained by the cells is not yet known. Collagen fibrils have been shown to pass through this zone with a predominantly radial orientation (Aspden & Hukins, 1981*a*, *b*) although not necessarily as continuous fibres, and the position of the calcified front appears to be a function of the joint and the species. It is not obvious why there should be a thicker layer than normal in the OP group though this could be a response to altered loading caused by a reduction in the bone plate thickness. The absence of calcified cartilage in the OA group is to be expected as these patients all exhibited advanced stages of the disease. This results in erosion of the cartilage down to the bone and remodelling of the bone itself, which together would effectively remove the calcified layer.

The EPMA results confirm that there are no differences in the stoichiometry of the mineral between any of the patient groups; the calcium:phosphorus ratio is always that expected of hydroxyapatite. Expressing the data as percentages of the oxides shows how much of the material is occupied by each stoichiometric grouping and so, by subtraction, what is not accounted for. The lower oxide contents found in the superior region of the OA femoral heads may be a reflection of the greater porosity apparent visually, though it is not clear why this was reduced in only the superior region whereas the visual appearance of the superior and inferior portions could not be readily distinguished. Whether these represent an altered crystallinity, an increase in canaliculi or an altered collagen-mineral morphology we are currently investigating.

Taken overall, the subchondral bone plate from the OA group shows more differences from normal than does that from the OP group. Apart from the increased quantity of bone, which was to be expected, the gross appearance of the fracture surfaces and the underlying trabeculae, the greater evidence of resorption pits and the altered amount of mineral are all consistent with the hypothesis that there is a primary defect in the regulation of bone in osteoarthritis and that these changes are not easily explained as a secondary consequence of the loss of articular cartilage.

ACKNOWLEDGEMENTS

We thank the Medical Research Council of Great Britain and the Sir Halley Stewart Trust for financial support. We are grateful to Dr W. J. McHardy, Dr D. W. Gregory and E. McMurray for pilot studies using BSE imaging and EPMA and to the Orthopaedic surgeons in Aberdeen for kindly making tissue available from their patients.

REFERENCES

AMIR G, PIRIE CJ, RASHAD S, REVELL PA (1992) Remodelling of subchondral bone in osteoarthritis: a histomorphometric study. *Journal of Clinical Pathology* **45,** 990–992.

ASPDEN RM, HUKINS DWL (1981*a*) Collagen organisation in articular cartilage determined by X-ray diffraction and its relationship to tissue function. *Proceedings of the Royal Society* **B212,** 299–304.

ASPDEN RM, HUKINS DWL (1981*b*) Calcification of the deep zone in pig femoral head cartilage. *Experientia* **37**, 1333.

BAILEY AJ, MANSELL JP (1997) Do subchondral bone changes exacerbate or precede articular cartilage destruction in osteoarthritis of the elderly? *Gerontology* **43**, 296–304.

BJÖRKSTRÖM S, GOLDIE IF (1982) Hardness of the subchondral bone of the patella in the normal state, in chondromalacia and in osteoarthrosis. *Acta Orthopaedica Scandinavica* **53**, 451–462.

BOYDE A, MACONNACHIE E, REID SA, DELLING G, MUNDY GR (1986) Scanning electron microscopy in bone pathology: review of methods, potential and applications. *Scanning Electron Microscopy* 1537–1554.

CARLSON CS, LOESER RF, PURSER CB, GARDIN JF, JEROME CP (1996) Osteoarthritis in cynomolgus macaques III: effects of age, gender, and subchondral bone thickness on the severity of disease. *Journal of Bone and Mineral Research* **11**, 1209–1217.

CHAI BF, TANG XM, LI H (1991) Scanning electron microscopic study of subchondral bone tissues in osteoarthritic femoral head. *Chinese Medical Journal* **104**, 503–509.

CHRISTENSEN P, KJAER J, MELSEN F et al. (1982) The subchondral bone of the proximal tibial epiphysis in osteoarthritis of the knee. *Acta Orthopaedica Scandinavica* **53**, 889–895.

CLARK JM, HUBER JD (1990) The structure of the human subchondral plate. *Journal of Bone and Joint Surgery* **72-B**, 866–873.

DEDRICK DK, GOLDSTEIN SA, BRANDT KD, O'CONNOR BL, GOULET RW, ALBRECHT M (1993) A longitudinal study of subchondral plate and trabecular bone in cruciate deficient dogs with osteoarthritis followed up for 54 months. *Arthritis and Rheumatism* **36**, 1460–1467.

DEQUEKER J, MOKASSA L, AERSSENS J (1995) Bone density and osteoarthritis. *Journal of Rheumatology* **22**, 98–100.

ECKSTEIN F, MILZ S, ANETZBERGER H, PUTZ R (1998) Thickness of the subchondral mineralised tissue zone (SMZ) in normal male and female and pathological patellae. *Journal of Anatomy* **192**, 81–90.

GEVERS G, DEQUEKER J, GEUSENS P, NYSSEN-BEHETS C, DHEM A (1989) Physical and histomorphological characteristics of iliac crest bone differ according to the grade of osteoarthritis at the hand. *Bone* **10**, 173–177.

HODGE WH, FIJAN RS, CARLSON KL, BURGESS RG, HARRIS WH, MANN RW (1986) Contact pressures in the human hip joint measured in vivo. *Proceedings of the National Academy of Sciences of the USA* **83**, 2879–2883.

JONES SJ, BOYDE A (1993) Histomorphometry of Howship's lacunae formed in vivo and in vitro: depths and volumes measured by scanning electron and confocal microscopy. *Bone* **14**, 455–460.

JONES SJ, BOYDE A, ALI NN (1984) The resorption of biological and nonbiological substrates by cultured avian and mammalian osteoclasts. *Anatomy & Embryology* **170**, 247–256.

KAMIBAYASHI L, WYSS UP, COOKE TDV, ZEE B (1995*a*) Changes in mean trabecular orientation in the medial condyle of the proximal tibia in osteoarthritis. *Calcified Tissue International* **57**, 69–73.

KAMIBAYASHI L, WYSS UP, COOKE TDV, ZEE B (1995*b*) Trabecular microstructure in the medial condyle of the proximal tibia of patients with knee osteoarthritis. *Bone* **17**, 27–35.

LEES S (1988) Sonic velocity and the ultrastructure of mineralised tissues. In *Calcified Tissues* (ed. Hukins DWL), pp. 121–152. London: Macmillan.

LEREIM P, GOLDIE I, DALBERG E (1974) Hardness of the subchondral bone of the tibial condyles in the normal state and in osteoarthritis and rheumatoid arthritis. *Acta Orthopaedica Scandinavica* **45**, 614–627.

LI B, ASPDEN RM (1997*a*) Mechanical and material properties of the subchondral bone plate from the femoral head of patients with osteoarthritis or osteoporosis. *Annals of the Rheumatic Diseases* **56**, 247–254.

LI B, ASPDEN RM (1997*b*) Composition and mechanical properties of cancellous bone from the femoral head of patients with osteoporosis or osteoarthritis. *Journal of Bone and Mineral Research* **12**, 641–651.

MBUYI-MUAMBA JM, DEQUEKER J (1984) Chemical composition of normal and osteoarthrotic cancellous bone of the femoral head. *Archives of Orthopaedic and Traumatic Surgery* **102**, 267–272.

MEACHIM G, STOCKWELL RA (1979) The matrix. In *Adult Articular Cartilage* (ed. Freeman MAR), pp. 1–67. London: Pitman Medical.

MENTE PL, LEWIS JL (1994) Elastic modulus of calcified cartilage is an order of magnitude less than that of subchondral bone. *Journal of Orthopaedic Research* **12**, 637–647.

MILZ S, PUTZ R (1994) Quantitative morphology of the subchondral plate of the tibial plateau. *Journal of Anatomy* **185**, 103–110.

MILZ S, ECKSTEIN F, PUTZ R (1995) The thickness of the subchondral plate and its correlation with the thickness of the uncalcified articular cartilage in the human patella. *Anatomy & Embryology* **192**, 437–444.

MURALI SR, PORTER RW, GREGORY DW, MARSHALL D, ASPDEN RM, McHARDY WJ (1994) New bone formation in an osteoporotic patient treated by intraosseous injection of bioactive materials. *Cells & Materials* **4**, 337–346.

OETTMEIER R, AROKOSKI J, ROTH AJ, HELMINEN HJ, TAMMI M, ABENDROTH K (1992) Quantitative study of articular cartilage and subchondral bone remodelling in the knee joint of dogs after strenuous running training. *Journal of Bone and Mineral Research* **7**, S419–S424.

PETERSSON IF, BOEGÅRD T, SVENSSON B, HEINEGÅRD D, SAXNE T (1998) Changes in cartilage and bone metabolism identified by serum markers in early osteoarthritis of the knee joint. *British Journal of Rheumatology* **37**, 46–50.

RADIN EL, ROSE RM (1986) The role of subchondral bone in the initiation and progression of cartilage damage. *Clinical Orthopaedics and Related Research* **213**, 34–40.

REDLER I, MOW VC, ZIMNY ML, MANSELL J (1975) The ultrastructure and biomechanical significance of the tidemark of articular cartilage. *Clinical Orthopaedics and Related Research* **112**, 357–362.

SHIMIZU M, TSUJI H, MATSUI H, KATOH Y, SANO A (1993) Morphometric analysis of subchondral bone of the tibial condyle in osteoarthrosis. *Clinical Orthopaedics and Related Research* **293**, 229–239.

SIMKIN PA, HESTON TF, DOWNEY DJ, BENEDICT RS, CHOI HS (1991) Subchondral architecture in bones of the canine shoulder. *Journal of Anatomy* **175**, 213–227.

THOMAS DB, DANIEL TS (1983) *In vitro* contact stress distributions in the natural human hip. *Journal of Biomechanics* **16**, 373–384.

WALTON M, ELVES MW (1979) Bone thickening in osteoarthrosis. Observations of an osteoarthrosis–prone strain of mouse. *Acta Orthopaedica Scandinavica* **50**, 501–506.